MODEL OF MULTI-BAND OFDM INTERFERENCE ON BROADBAND QPSK RECEIVERS

Celestino A. Corral, Shahriar Emami and Gregg Rasor

Freescale Semiconductor
8000 W. Sunrise Blvd.
Plantation, FL 33322

ABSTRACT

A model for multi-band orthogonal frequency division multiplex (MB-OFDM) interference on in-band broadband uncoded QPSK receivers is provided. Multi-band OFDM results in periodic gated noise with power scaled to equal the total power of AWGN over the entire hop time. Since MB-OFDM can have high peak-to-average power (PAP), its impulsive characteristics are captured by the model as a function of the hop depth. Based on the proposed model, it is shown that MB-OFDM is a more harmful interference than ungated AWGN for the same effective isotropic radiated power (EIRP).

1. INTRODUCTION

Ultra-wideband (UWB) has emerged as an important technology for short-range high data rate wireless communication. With the FCC approval for unlicensed UWB communications in the 3.1–10.6 GHz band, UWB has become the featured alternative physical layer for IEEE 802.15.3a wireless personal area network (WPAN) standard and is being considered for TG4a as well.

One of the proposed physical layers for 802.15.3a is multi-band orthogonal frequency division multiplex (MB-OFDM), consisting of 128 subcarriers over a 528 MHz bandwidth that is hopped based on a time-frequency code [1]. MB-OFDM mates the advantages of OFDM as described in [2] with frequency hopping for multi-user support. Frequency hopping also mitigates some of the limitations of the implementation technology; CMOS is currently incapable of fully exploiting the FCC allocated 3.1–10.6 GHz spectrum in full OFDM form at high data rates.

In this paper we present a series of simulations and analyses to derive a model for the impact of MB-OFDM interference on in-band high data rate QPSK receivers. It is shown that MB-OFDM is actually bounded by periodic gated AWGN and worst-case impulsive OFDM. The resulting model captures the effect as a function of hop depth and can be used to estimate the uncoded symbol error rate of broadband QPSK receivers subjected to MB-OFDM in-band interference.

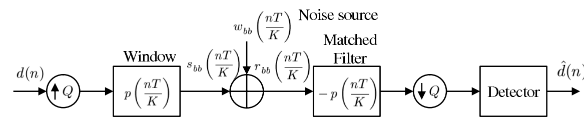

Fig. 1. QPSK receiver implemented in MATLAB for performing the interference analyses.

2. FIRST-ORDER PERIODICALLY GATED AWGN MODEL

Multi-band OFDM modulation hops in the UWB spectrum so the power spectral density (PSD) is averaged over time. In order to equate the PSD of gated and hopped MB-OFDM with the PSD of ungated and unhopped DS-UWB (which is modeled as an AWGN process), we equate the total powers of each as considered in [3]. Since MB-OFDM interference is present $1/N$ of the time for hop depth N, the average power seen by the receiver is equal to AWGN over the entire hop depth N. This scaling of MB-OFDM results in a perceived higher peak power as observed by the victim receiver because the power is concentrated over a smaller bandwidth than a DS-UWB system. However, as we have normalized everything to power, both systems exhibit identical range *a forteriori*.

The victim receiver is a video satellite receiver employing QPSK modulation with a symbol rate as high as 27.5 Msym/sec (comparable to an international satellite service feed such as Dubai EDTV at 4020 MHz). A baseband QPSK simulator was implemented in MATLAB assuming perfect synchronization and phase estimation. The output is extracted at the optimum sampling of the rectangular windowed matched filter output as shown in Figure 1.

The temporal response of the band-pass filter exhibits fast rise time [3] and the filter bandwidth is broad enough so that the interference appears as thermal noise [4]. To simplify the analysis, we remove the front-end filter from the simulation and scale the power of MB-OFDM so that its average power is equal to that of AWGN over all the symbols considered. For the simulations, a stream of 1000 symbols and

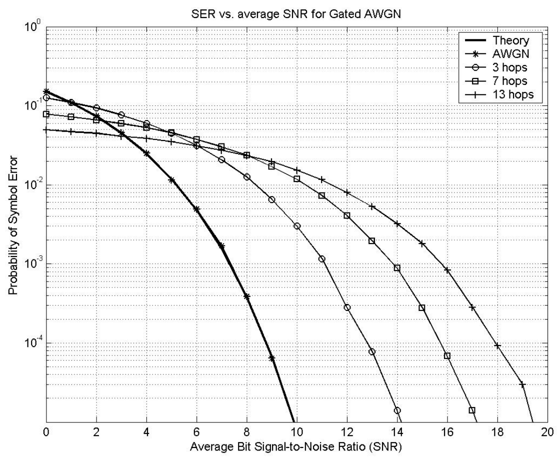

Fig. 2. Probability of symbol error versus average E_b/N_o for gated noise at different hop lengths. Theoretical results are also provided.

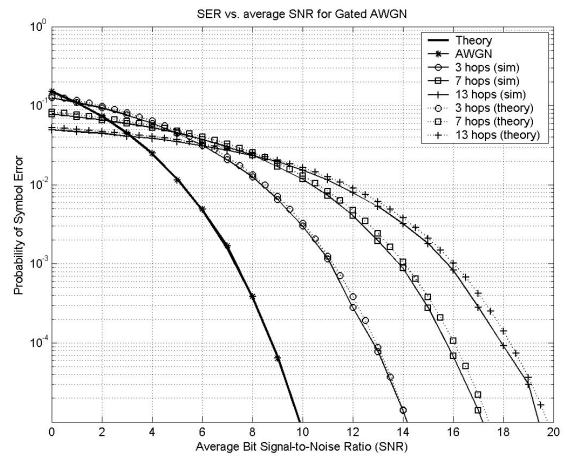

Fig. 3. Probability of symbol error versus average E_b/N_o for gated noise at different hop lengths. Theoretical results are also provided (dashed lines).

500 packets were implemented over $0 \leq E_b/N_o \leq 30$ dB. The simulated system was uncoded.

The plot of Figure 2 shows the simulated probability of a symbol error for the QPSK system under periodic and scaled gated noise conditions. The AWGN simulation was calibrated to the theoretical curve shown in the plot. All other simulations are made relative to the calibrated system. As is evident, as the hop interval between gated noise increases, the symbol error rate rises significantly. For 3 hops, SER ≈ 3 dB worse than theory at 10^{-2} and > 4 dB worse at 10^{-4}; for 7 hops we have 5 and 7 dB from theory, respectively; for 13 hops we have 6 and 8 dB from theory, respectively. Hence, for the case where the noise corrupts a number of QPSK symbols at high symbol rates, gated noise with scaled power results in significant QPSK system degradation at average SNR > 4 dB.

The poor QPSK receiver performance for gated noise is due to the equating of the EIRP. Since the gated periodic AWGN average power is made equal to the AWGN average power over the total hop time, the net effect of the gated interference is a corresponding drop in the observed bit energy by the receiver. Hence, the periodic gated noise phenomenon is quasi-fading in character, introducing significant errors. We now seek to quantify this phenomenon.

To proceed, let us note that the probability of symbol error P_{symbol} for a coherently detected QPSK signal is related to the probability of a bit error P_e as [5]

$$P_{symbol} = 1 - [1 - P_e]^2, \quad P_e = Q\left(\sqrt{\frac{2E_b}{N_o}}\right) \tag{1}$$

where E_b is the signal energy per binary symbol normalized to a 1-Ω load (in V), N_o is the single-sided noise power spectral density (in W/Hz), and

$$Q(x) = \frac{1}{2\pi}\int_x^{\infty} e^{-u^2/2}du = \frac{1}{2}\text{erfc}(x/\sqrt{2}) \tag{2}$$

We can work with P_e in (1) to generate the plots.

In the gated noise condition, we have a noise source interfering periodically over a portion of time, with a duty cycle

$$\rho = \frac{N_p}{N_p + N_s} \leq 1 \tag{3}$$

where N_p is the time the interferer is present, and N_s is the time the interferer is silent. The total probability of error is therefore

$$P_e = \rho P_{ep} + (1-\rho)P_{es} \tag{4}$$

where P_{ep} is the probability of erro with the noise present, and P_{es} is the probability of erro when the noise is silent. When the noise is silent, there is no interference and the error is $P_{es} = 0$. In addition, the noise power, when present, is scaled by the inverse of the duty cycle as $1/\rho$, equating the total power of AWGN over the time $N_p + N_s$. Hence,

$$P_{ep} = Q\left(\sqrt{\frac{2E_b}{N_o/\rho}}\right) = Q\left(\sqrt{\rho\frac{2E_b}{N_o}}\right) > Q\left(\sqrt{\frac{2E_b}{N_o}}\right) \tag{5}$$

and there is a rise in the probability of error since $\rho < 1$ from (3). This error emerges from the scaling of the signal energy by the duty cycle and is equivalent to the periodic quasi-fading phenomenon explained earlier.

Since the interference is periodic, its presence is determined by the duty cycle ρ. Thus, the probability of error occurs only during the time the interference is present. The actual probability of error is therefore

$$\tilde{P}_e = \rho P_e \tag{6}$$

and this is substituted into (1). A plot of the theoretical results is provided in Figure 3 as superimposed on the results of Figure 2. The results are virtually identical, showing that the gated AWGN model is suitable for capturing the interference of MB-OFDM under these conditions.

3. SECOND-ORDER MB-OFDM INTERFERENCE MODEL

Multi-band OFDM is based on OFDM which can exhibit impulsive characteristics. In particular, for OFDM PAP $= 10\log(N)$ where N is the number of subcarriers. For a MB-OFDM signal, the PAP can be as high as 21 dB for 128 subcarriers. However, the frequency hopping corresponds to an equivalent time gating of the symbol relative to the received input. Therefore, if the average of the symbol is some value A, then for N hops, the victim receiver sees an average $\tilde{A} = A/N$ over the full hop length, yielding

$$\text{PAP}_{actual} = N\text{PAP}_{symbol} \tag{7}$$

For $N = 3,\ 7,\ 13$, the lowest PAP for a given gated OFDM symbol is 4.77, 8.45, and 11.14 dB (i.e., $10\log(N)$), respectively. For a combination of the worst-case PAP under the longest hop sequence, the actual PAP can be as high as 32 dB! Hence, the MB-OFDM signal can appear highly impulsive to a receiver under high SNR and be more destructive to a victim receiver.

To simulate the effects of the impulsive nature of MB-OFDM, a single high PAP MB-OFDM signal (all equal zero symbols) was generated with power matched to AWGN over all hops. In addition, the multi-band OFDM signal was generated with its average power matched to AWGN over all hops. Figure 4 shows the resulting plots of the symbol error rate for all these cases, including periodically gated AWGN of the previous section, for hop depth $N = 3$. It is evident that MB-OFDM performance is bounded below by gated AWGN (absolutely Gaussian) and worst-case impulsive OFDM (absolutely impulsive). Hence, we are led to the modeling of MB-OFDM as a combination of Gaussian and impulsive noise.

To derive the model, we turn to the class A or "narrowband" interference model with finite impulse duration T_I conforming to the condition [6]

$$T_I \Delta f_R \gg 1 \tag{8}$$

where Δf_R is the receiver bandwidth. For a purely Poisson process, class A noise yields "gaps" in time; i.e., non-zero probability of time during which there is no interference in

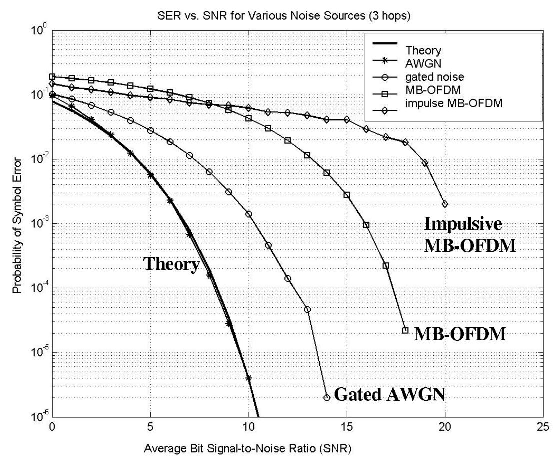

Fig. 4. Probability of symbol error versus average E_b/N_o for all noise sources at 3 hop depth.

the receiver [8]. Due to the long MB-OFDM symbol (240 nsec without guard interval) and the wide bandwidth of the victim receiver (40 MHz), (8) holds and the class A model can be employed.

The average symbol error rate for the class A model consisting of the summation of impulsive and Gaussian noise is given by [7]

$$P_{I+G}(e) \approx \frac{2(M-\sqrt{M})}{M} e^{-A} \cdot \sum_{j=0}^{\infty} \frac{A^j}{j!} \operatorname{erfc}\left(\frac{\sqrt{\text{CNR}\cdot\text{PF}^{(M)}}}{\sqrt{2}(\sqrt{M}-1)\sigma_j}\right) \tag{9}$$

where $A \le 1$ is the impulsive index, i.e., the product of the received average number of impulses in a second and the duration of the impulse. The value of A measures the temporal overlap among waveforms of interfering signals; large A means large overlap with corresponding approach to Gaussian distribution; small A means highly impulsive or "structured" interference. In (9), M is the modulation level for M-ary QAM, CNR is the carrier-to-noise ratio given by

$$\text{CNR} = \frac{S^2/2N_t}{\text{PF}^{(M)}} \tag{10}$$

with S being the peak signal envelope, $N_t = \sigma_G^2 + \sigma_I^2$ is the total noise power consisting of the Gaussian noise component σ_G^2 and the impulsive noise component σ_I^2, $\text{PF}^{(M)}$ is the peak factor (peak-to-average) of the M-ary QAM symbol. The value

$$\sigma_j = \frac{(j/A + \Gamma')}{(1+\Gamma')} \tag{11}$$

is the variance due to the impulsive index and the ratio $\Gamma' = \sigma_G^2/\sigma_I^2$.

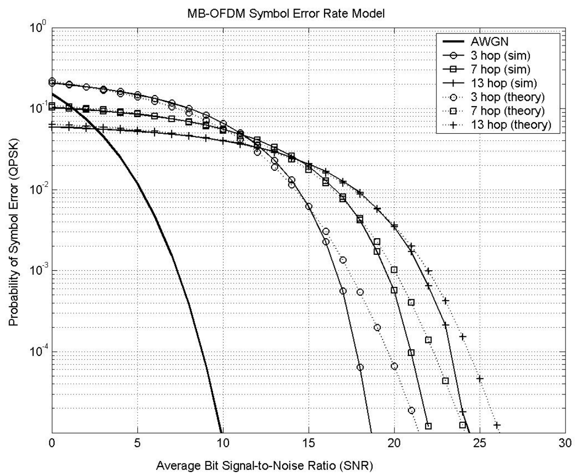

Fig. 5. Probability of symbol error versus average E_b/N_o for MB-OFDM and class A model incorporating Gaussian and impulsive characteristics.

The class A model captures the summation of probability density functions (pdf) of the contributing interference sources as Gaussian with varying standard deviations. A logical approach to deriving the model is to observe that the impulsive index consists of a periodic component proportional to the hop depth, i.e., $A \propto 1/N$. As the impulsive index becomes smaller, the noise impulsiveness becomes stronger, leading to larger performance degradation. As $A \to 1$, the impulsive noise occurs continuously, and the as the mean power ratio Γ' increases, the interference becomes more Gaussian [7]. Thus, to model the impulsive potential of MB-OFDM, $\Gamma' \propto 1/N$ should also hold.

By considering the SNR as opposed to the CNR directly into the formulation of (9) and performing a curve fit to the simulated results for MB-OFDM, the parameters are

$$A = \Gamma' = 0.5N, \quad P_e = 2P_{I+G}(e) \tag{12}$$

Fitting these values into (9) with SNR as the parameter we obtain the plots in Figure 5. Since A is rather small as N increases, the impulsive characteristic is emphasized. This also results in an evaluation of (9) for small values of j, reducing the computational load. The model is adequate for uncoded symbol error rates up to 10^{-4}.

Multi-band OFDM can be modeled by a combination of Gaussian and impulsive interference contributors with closed-form average symbol error rate given by the class A model of (9) with the values given in (12). This model confirms that the periodic gating introduces greater impulsive characteristics and results in degraded receiver performance relative to ungated AWGN.

4. CONCLUSIONS

Multi-band OFDM consists of OFDM symbols that hop into different frequency bands depending on some time-frequency code; an in-band broadband receiver perceives MB-OFDM as periodic gated interference and is modeled as such. However, to equate the range of MB-OFDM with a DS-UWB source modeled by an AWGN process, the average power of the OFDM symbol was scaled relative to the average power of AWGN over the total hop time. The results show that MB-OFDM interference is more damaging to in-band high data rate QPSK receivers under these conditions. A model for the multi-band OFDM interference was derived based on the combination of AWGN and impulsive characteristics and shown to accurate estimate symbol error rates as a function of hop depth N.

5. REFERENCES

[1] "TI Physical Layer Proposal for IEEE 802.15 Task Group 3a," *IEEE P802.15 Working Group for Wireless Personal Area Networks (WPANs)*, Doc. P802.15-03/142r1, May 12, 2003.

[2] J. A. C. Bingham, "Multicarrier modulation for data transmission: An idea whose time has come," *IEEE Commun. Mag.*, vol. 28, pp. 5–14, May 1990.

[3] C. A. Corral, S. Emami, and G. Rasor, "In-band interference of multi-band OFDM systems," to be published in *IEEE Int. Symp. Spread Spectrum Systems Tech.*, 2004.

[4] J. Brandão, "Interference effect on the performance of PSK and QAM systems," *IEE Proceedings I*, vol. 138, pp. 331–337, Aug. 1991.

[5] J. G. Proakis, *Digital Communications*, 4th Ed., Boston, MA: McGraw-Hill, 2001.

[6] D. Middleton, "Non-Gaussian noise models in signal processing for telecommunications: New methods and results for class A and class B noise models," *IEEE Trans. Inform. Theory*, vol. 45, pp. 1129–1149, May 1999.

[7] J-S. Seo, S-J. Cho, and K. Feher, "Impact of non-Gaussian impulsive noise on the performance of high-level QAM," *IEEE Trans. Electromagn. Compat.*, vol. 31, pp. 177–180, May 1989.

[8] A. D. Spaulding and D. Middleton, "Optimum reception in an impulsive interference environment: Coherent detection," *IEEE Trans. Commun.*, vol. COM-25, pp. 910–923, Sept. 1977.